© 2005 International Society for Analytical Cytology

DNA Labeling in Living Cells

Robert M. Martin,[1] Heinrich Leonhardt,[1,2] and M. Cristina Cardoso[1]*

[1]Max Delbrück Center for Molecular Medicine, Berlin, Germany

[2]Ludwig Maximilians University Munich, Department of Biology II, Planegg-Martinsried, Germany

Received 26 January 2005; Revision Received 9 May 2005; Accepted 28 June 2005

Background: Live cell fluorescence microscopy experiments often require visualization of the nucleus and the chromatin to determine the nuclear morphology or the localization of nuclear compartments.

Methods: We compared five different DNA dyes, TOPRO-3, TOTO-3, propidium iodide, Hoechst 33258, and DRAQ5, to test their usefulness in live cell experiments with continuous imaging and photobleaching in widefield epifluorescence and confocal laser scanning microscopy. In addition, we compared the DNA stainings with fluorescent histones as an independent fluorescent label to mark chromatin.

Results: From the dyes tested, only Hoechst and DRAQ5 could be used to stain DNA in living cells. However, DRAQ5 had several advantages, namely low photobleaching, labeling of the chromatin compartments comparable to that of H2B-GFP fusion proteins, and deep red excitation/emission compatible with available genetically encoded fluorescent proteins such as C/G/YFP or mRFP.

Conclusions: The DNA dye DRAQ5 is well suited for chromatin visualization in living cells and can easily be combined with other fluorophores with blue to orange emission. © 2005 Wiley-Liss, Inc.

Key terms: DNA dyes; DRAQ5; chromatin; nuclear structure; live cell imaging; fluorescence microscopy

In the fields of biological research and medical diagnosis, staining techniques and chemicals to visualize DNA or chromatin with fluorescence microscopy are widely used and have been of high importance for decades (1,2). Many of these dyes are restricted to fixed cell samples and show only roughly the distribution of nuclei in cells and tissues (3). Further, fixation of cells often produces undesired artifacts (4). DNA dyes for live cell fluorescence microscopy should match the criteria of low cytotoxicity and phototoxicity combined with low photobleaching (5). In addition, a suitable live cell DNA dye should specifically label deoxyribonucleic acids stoichiometrically and should be easy to combine with commonly used autofluorescent proteins such as CFP, GFP, YFP, or mRFP (6). Several of the available dyes such as TOPRO, the TOTO dye family, ethidium bromide, and propidium iodide (PI) require permeabilization or similar membrane disruptive methods to label the DNA efficiently (3). Further, several of these dyes bind strongly to RNA requiring a RNAse treatment of fixed and permeabilized samples (3,7). The dyes 4′,6-diamidino-2-phenylindole (DAPI) and Hoechst are widely used DNA-specific dyes, which emit blue fluorescence under ultraviolet (UV) illumination when bound to DNA. Because UV light damages cellular DNA and other components, the use of Hoechst in live cell microscopy is very restricted in time (1,8). In addition, DAPI and Hoechst have a preference to bind to A/T-rich DNA sequences and highlight a subset of the genome. Thus, the use of these dyes is impossible in long-term live cell experiments and they also do not necessary reflect quantitative variations in DNA condensation. Other approaches such as expression of fluorescent histone fusions, albeit an extraordinarily useful tool in cell biology, require prior transfection of cells and a several-hour period until the microscopic visualization can start (9). In addition, several cell types, in particular primary cultures, are very difficult or impossible to transfect (2). In the present study, we compared DNA dyes with chromatin labeling using fluorescent histones to identify a dye that could be used in living cells and could reflect stoichiometrically the spatial distribution of DNA content in living cell nuclei.

MATERIALS AND METHODS

Cell Culture and Viability

Human HeLa cells and HeLa H2B-GFP stable cell line (9) were cultivated in Dulbecco's Modified Eagle's Medium with 10% fetal calf serum plus 5 mM L-glutamine and 5 μg/ml gentamicin. Mouse C2C12 myoblasts and the C2C12 GFP-PCNA stable cell line (10) were grown in Dulbecco's Modi-

Contract grant sponsor: Deutsche Forschungsgemeinschaft.

*Correspondence to: M. Cristina Cardoso, Max Delbrück Center for Molecular Medicine, Franz-Volhard-Klinik, Wiltbergstrasse 50, 13125 Berlin, Germany.

E-mail: cardoso@mdc-berlin.de

Published online 4 August 2005 in Wiley InterScience (www.interscience.wiley.com).

DOI: 10.1002/cyto.a.20172

fied Eagle's Medium with 20% fetal calf serum and the same additives. For live cell microscopy cells were seeded into four-well LabTek glass-bottom chambers (Nalge Nunc International, Naperville, IL, USA) and covered with the desired growth medium the day before.

The effect of DRAQ5 on cell viability was assayed by plating equal numbers of cells and 1 day later adding or not adding the dye to the medium. The next day, cells were trypsinized and counted using a hemacytometer. Experiments were repeated twice and cells were counted in duplicate dishes. To analyze the effect of DRAQ5 on cell cycle progression, the DNA content of HeLa cells treated in the same manner was analyzed after methanol fixation by PI staining in the presence of RNAse as described before (10) followed by flow cytometry (FACScalibur, BD Biosciences, Heidelberg, Germany). Ten runs with 10^4 cells each were analyzed using ModFit 3.0 software and the mean values of cells in each cell cycle stage were calculated for control and DRAQ5 incubated cells.

DNA Stainings

Cells were grown to 50% confluency on 12-mm Ø glass coverslips. The samples were fixed for 10 min with 3.7% formaldehyde (Fluka Chemie GmbH, Buchs, Switzerland) in phosphate buffered saline; for staining with PI, TOPRO-3 and TOTO-3 were permeabilized for 10 min with 0.25% Triton X-100. RNAse digestion was performed with 200 μg/ml RNAse for 30 min (Sigma, St. Louis, MO, USA). The DNA dyes were applied at the concentrations listed in Table 1 for 5 to 10 min. The coverslips were rinsed with phosphate buffered saline between each incubation step and at the end mounted with Moviol.

For live cell experiments, cells were grown in LabTek chambers and the growth medium was supplied with 1 μM DRAQ5 or 1.6 μM Hoechst 33258 (final concentrations) for 5 min before image acquisition.

DRAQ5 was purchased from Biostatus Limited (Leicestershire, UK), TOPRO-3 and TOTO-3 were obtained from Molecular Probes (Leiden, The Netherlands), Hoechst 33258 was obtained from Hoefer Scientific Instruments (San Francisco, CA, USA), and PI was obtained from Sigma.

Fluorescence Microscopy

Live cell microscopy was performed with an objective heated to 37°C using a confocal laser scanning microscope (LSM510Meta, Carl Zeiss, Jena, Germany) equipped with argon ion and HeNe lasers. Fixed cells were imaged on the same confocal microscope (Fig. 1A) and on a widefield epifluorescence microscope (Zeiss Axioplan 2) equipped with a 100-W mercury lamp. The latter was used for general bleaching analysis (Table 1). In the live cell photobleaching experiments (Fig. 3A), cells were continuously imaged over time. Excitation, beamsplitters, and emission filters used for imaging of the various fluorophores are listed in Table 2.

Image Analysis

Image analysis (Fig. 3A) was carried out by selecting the nuclei in the images and determining the mean fluorescence intensity of all the pixels selected. Subsequently, the relative fluorescence intensity was calculated by setting the mean fluorescence intensity of the first image in a time series to 100%.

The line scan and colocalization analysis (Pearson's coefficient; Fig. 3B–E) and the above image analysis were performed with Zeiss LSM Image examiner 3.2 and Origin 7.5 software (Origin Lab Corp., North Hampton, MA, USA).

RESULTS

We compared five different DNA binding agents for their ability to fluorescently label nuclear DNA in living cells. In addition, we tested whether they precisely represent the chromatin content in different nuclear compartments imaged by high-resolution confocal fluorescence microscopy. Further experiments were carried out to test the photobleaching behavior of the DNA dyes and the viability of cells in culture in the presence of the dye.

Figure 1A displays representative confocal optical sections of mitotic and interphase HeLa cells stably expressing H2B-GFP (9) and stained with the different dyes with and without RNAse treatment. From the five dyes tested, only Hoechst 33258 and DRAQ5 showed membrane-permeable properties and allowed the staining of DNA in living cells (Table 1 and Fig. 1A). The nucleic acid dyes PI, TOTO-3, and TOPRO-3 did not penetrate intact cellular

Table 1
Summary of Nucleic Acid Dyes Characteristics

	TOPRO-3	TOTO-3	Propidium Iodide	Hoechst 33258	DRAQ5
Excitation/emission maximum (nm)	642 / 661[a]	642 / 660[a]	535 / 617[a]	352 / 416[a]	647 / 670[b]
Cell permeable	−	−	−	+	+
Live/fixed cell application	−/+	−/+	−/+	+/+	+/+
DNA sequence specificity	no[a]	some CTAG preference[a]	no[a]	A/T preference[a]	no[b]
RNA staining	−	+	+	−	−
Bleaching behavior	Very fast (5–10 s)	Fast (20–30 s)	Slow (1–2 min)	Slow (1–2 min)	No bleaching observed
Working concentration	50 μM	1 μM	1.5 μM	1.6 μM	1 μM

[a]Molecular Probes.
[b]Biostatus Limited.

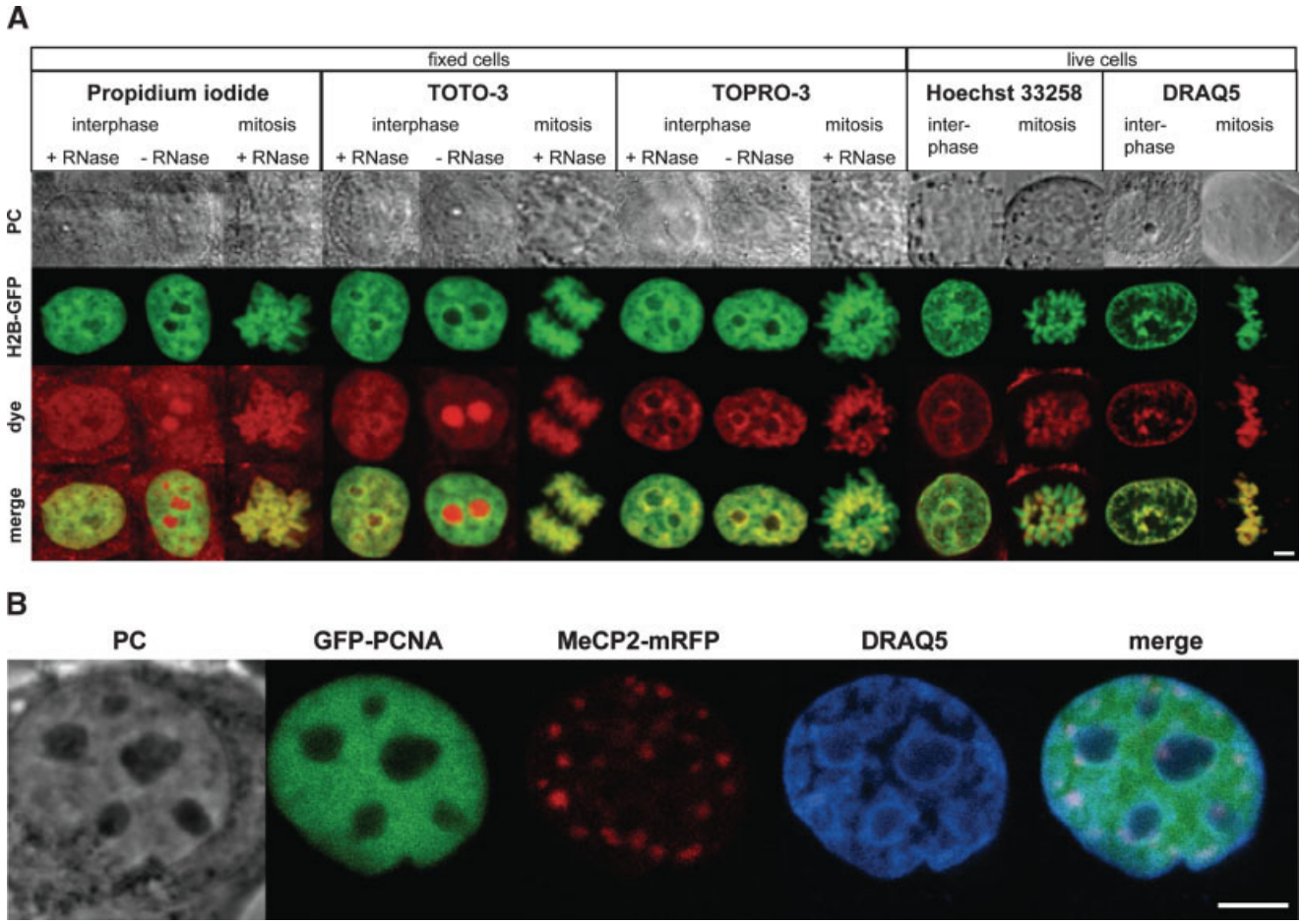

FIG. 1. **A:** Comparison of DNA staining by PI, TOTO-3, TOPRO-3, Hoechst 33258, and DRAQ5 with H2B-GFP chromatin labeling in HeLa cells. For all dyes the H2B-GFP chromatin label and DNA staining were imaged in interphase and mitotic cells. The three fixed-cell dyes TOTO-3, TOPRO-3, and PI were imaged with or without RNAse digestion. Dye concentrations are as listed in Table 1. For Hoechst and DRAQ5, only live cell images are shown. In all cases, confocal optical sections are presented with the corresponding phase contrast images. **B:** Combined imaging of DRAQ5 and two different autofluorescent proteins. Living C2C12 mouse myoblast cells expressing the cell cycle marker GFP-PCNA (10) and a protein (MeCP2-mRFP) that binds to pericentric heterochromatin were stained with DRAQ5. The latter also shows that DRAQ5, in contrast to Hoechst/DAPI dyes, does not preferentially stain this type of heterochromatin. The three different fluorophores were excited and detected independently (imaging conditions as listed in Table 2) and no cross-talk was observed. Scale bars = 5 μm.

membranes and their application was restricted to permeabilized cells (Fig. 1A). Although TOTO-3 and TOPRO-3 have fluorescence emission in the deep red spectral range, PI emits at wavelengths similar to those of mRFP or rhodamine and strongly compromises the simultaneous use of these fluorophores. Further, PI and TOTO-3 bind to cellular RNA as seen by the strong staining of the nucleolus and required an additional RNAse digestion (Fig. 1A).

Table 2
Summary of Imaging Conditions

Fluorophore	Excitation (nm)	Main beamsplitter (nm)	Secondary beamsplitter (nm)	Emission (nm)
LSM510Meta confocal microscope				
Hoechst 33258	2P 762[a]	KP 680	—	BP 435-485IR
GFP	488	UV/488/543/633	NFT 545	BP500-530IR
PI, mRFP	543	UV/488/543/633	NFT 545	BP585-615
DRAQ5, TOPRO-3, TOTO-3	633	UV/488/543/633	NFT 545	LP 650
Axioplan 2 widefield microscope				
Hoechst 33258	365/12	395	—	397LP
GFP	450–490	510	—	515-565BP
PI	530–585	600	—	615LP
DRAQ5, TOPRO-3, TOTO-3	572–625	645	—	660-710BP

[a]Two-photon excitation.

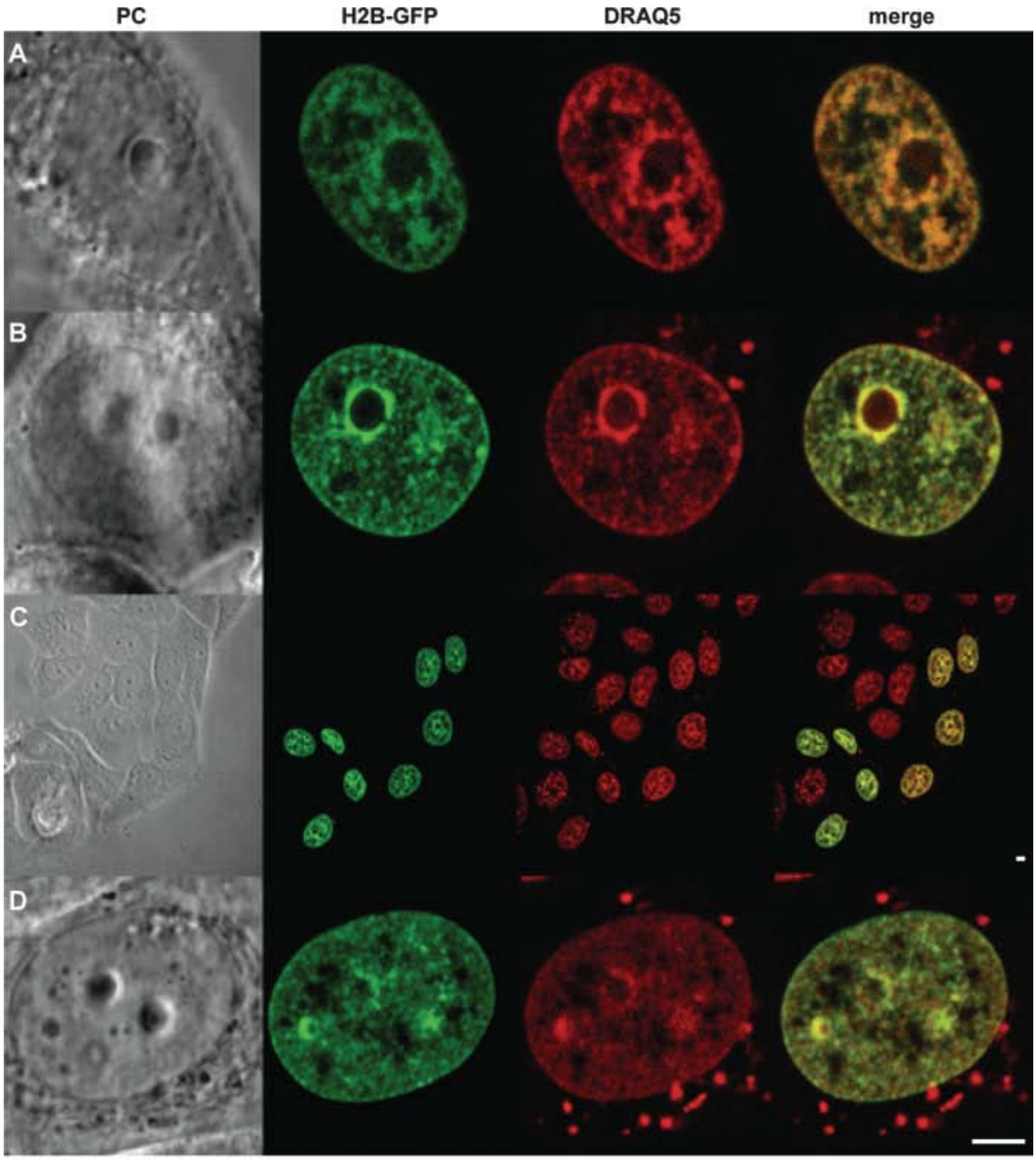
PC
H2B-GFP
DRAQ5
merge
A
B
C
D

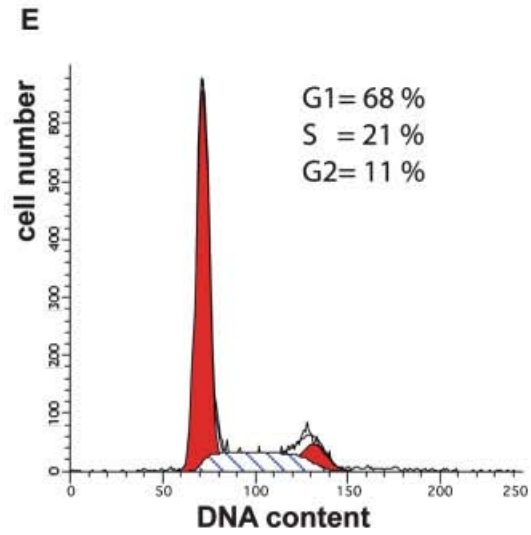
E
cell number
G1= 68 %
S = 21 %
G2= 11 %
0
50
100
150
200
250
DNA content

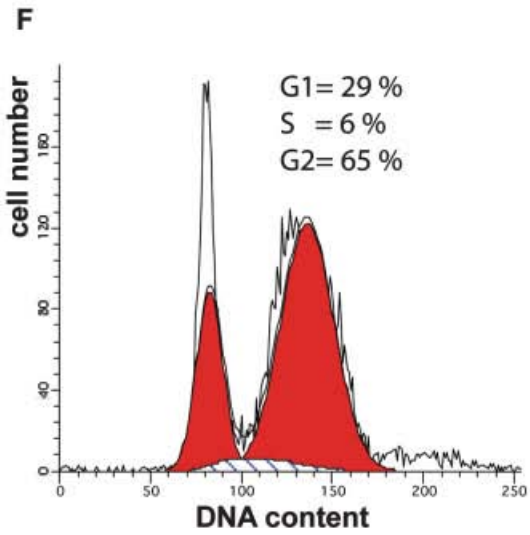
F
cell number
G1= 29 %
S = 6 %
G2= 65 %
0
50
100
150
200
250
DNA content

Only Hoechst 33258 and DRAQ5 could be used to label nuclear DNA in living cells (Fig. 1A). Both dyes were added to the growth medium and stained the nuclear DNA in 5 to 10 min. One major advantage of Hoechst 33258 is the easy combination with many other fluorescent dyes or proteins, from the green to the deep red spectral range of visible light. However, the Hoechst 33258 dye requires excitation with an UV light source or multiphoton laser excitation (Fig. 1A). The former produces additional problems including UV-induced cell damage that decreases cell viability and bleaching due to high-energy excitation light. A continuous imaging of Hoechst-stained living cells with 762-nm two-photon excitation resulted in very fast cell death (data not shown). The fluorescence signals from Hoechst 33258 and H2B-GFP showed a complete overlap but differed in the intensity of the chromatin compartments (Figs. 1A and 3D), which results from the Hoechst 33258 preference to bind to A/T-rich genomic DNA sequences, thereby highlighting some genomic sequences, e.g., pericentric heterochromatin in mouse cells (11).

In view of these caveats of the Hoechst/DAPI DNA dye family, we tested the recently described DNA intercalator DRAQ5 (12,13). The comparison of DRAQ5 nuclear DNA staining with H2B-GFP–labeled chromatin in live cells showed a costaining of the same nuclear regions and the chromosomes in mitotic cells (Fig. 1A). This nucleic acid dye was identified by directed derivatization of fluorescent anthraquinones, which are chemically related to the DNA intercalating anthracycline antibiotic and the anticancer drug mitoxanthrene (12,13). The name DRAQ5 stands for deep red fluorescing anthraquinone Nr. 5 and this compound is a membrane-permeable, DNA intercalating agent with an excitation at 647 nm but is also excitable at a broad range of wavelengths starting from 488 nm (13). These fluorescent properties make DRAQ5 potentially suited for use in combination with the available autofluorescent proteins. We directly tested this by adding DRAQ5 to living mammalian cells coexpressing nuclear mRFP and GFP fusion proteins. As shown in Figure 1B, no bleed-through between the different channels was apparent and the individual nuclear compartments were easy to distinguish and image.

To investigate the dynamics of uptake/labeling of DRAQ5 into living cells, we performed time-lapse fluorescence microscopy. The latter showed a rapid entry of DRAQ5 into the cells and binding to DNA by fluorescence enhancement upon DNA intercalation. The staining was already visible after 3 min and reached the equilibrium at 13 min (data not shown).

To assess the potential toxicity of this intercalating dye at the concentration used, we incubated cells in growth medium with DRAQ5 at a concentration of 1 μM continuously for 1 day (Fig. 2A-D) or for about 1 h followed by changing to growth medium without the dye and incubated the cells until the next day (data not shown). Both types of incubation with DRAQ5 over a 24-h period did not drastically affect cell viability. In the short DRAQ5 incubation experiment followed by 24-h growth medium incubation, the DRAQ5 signal intensity was decreased in the nuclei and cytoplasmic accumulations became visible (data not shown). In the continuous DRAQ5 incubation experiment, the nuclear DNA staining remained very strong 1 day later (Fig. 2C,D). We further tested the effect on cellular viability by plating equal numbers of cells, subjecting them to the 24-h DRAQ5 incubation scheme as before, and, 1 day later, trypsinizing and counting the number of cells. Compared with untreated cells in the same experiment, there were approximately 50% fewer cells after 24 h of DRAQ5 incubation. This was not due to cell death because the number of cells plated did not decrease and apoptotic cells were not apparent but likely lowered proliferation rate. To directly test this possibility, we performed the same 24-h DRAQ5 incubation scheme and analyzed the cell cycle progression by flow cytometric determination of the DNA content. The results clearly showed no sub-G1 DNA population of cells, which would be indicative of cell death, but a pronounced accumulation of cells in G2 phase (Fig. 2E,F).

Next we compared the photobleaching behavior of the different DNA dyes. Under continuous widefield epifluorescent excitation with a mercury lamp, we observed a fast bleaching of TOPRO-3 (after 5 to 10 s) and to some extent a slower bleaching of TOTO-3 (after 20 to 30 s; Table 1). Accordingly, this allows the acquisition of only one or two images with a laser scanning microscope before the fluorescent signals are bleached. The bleaching rates of PI and Hoechst 33258 were comparable to those of GFP and other more stable fluorophores with the fluorescence signal disappearing after 1 min (Table 1). Under these illumination conditions, DRAQ5 showed no detectable photobleaching. We then directly compared the photobleaching of DRAQ5 with GFP using a confocal laser scanning microscope. In time series, we were able to acquire about 120 images of DRAQ5-labeled nuclei of living HeLa H2B-GFP cells at a high magnification and resolution with minor bleaching, whereas the fluorescent histone label bleached away after about 60 images (Fig. 3A).

We tested whether DRAQ5 accurately reflects the DNA/chromatin distribution within the nucleus by correlating it with the H2B-GFP chromatin label. For this purpose, we

FIG. 2. Viability test for DRAQ5-stained cells. DRAQ5 was added to the growth medium of HeLa H2B-GFP cells and confocal images were acquired at different time points. **A:** A cell nucleus 5 min after application of the dye. The DNA in the cell nucleus is already stained with DRAQ5. **B:** The same can be seen 1 h later, with only a few additional cytoplasmic DRAQ5 signals. After 24 h the overview (**C**) and the magnified image of a nucleus (**D**) show that the cells are viable and appear morphologically unchanged. HeLa cells incubated (**F**) or not (**E**) for 1 day with DRAQ5 were methanol fixed and stained with PI followed by DNA content analysis by flow cytometry. DNA histograms were analyzed with ModFit software to determine the percentage of cells in the different cell cycle stages. Although 11% of the control cells were in G2/M, the cells incubated for 1 day with DRAQ5 at 1 μM showed a drastic accumulation in G2 phase (65% of all cells). Scale bar = 5 μm.

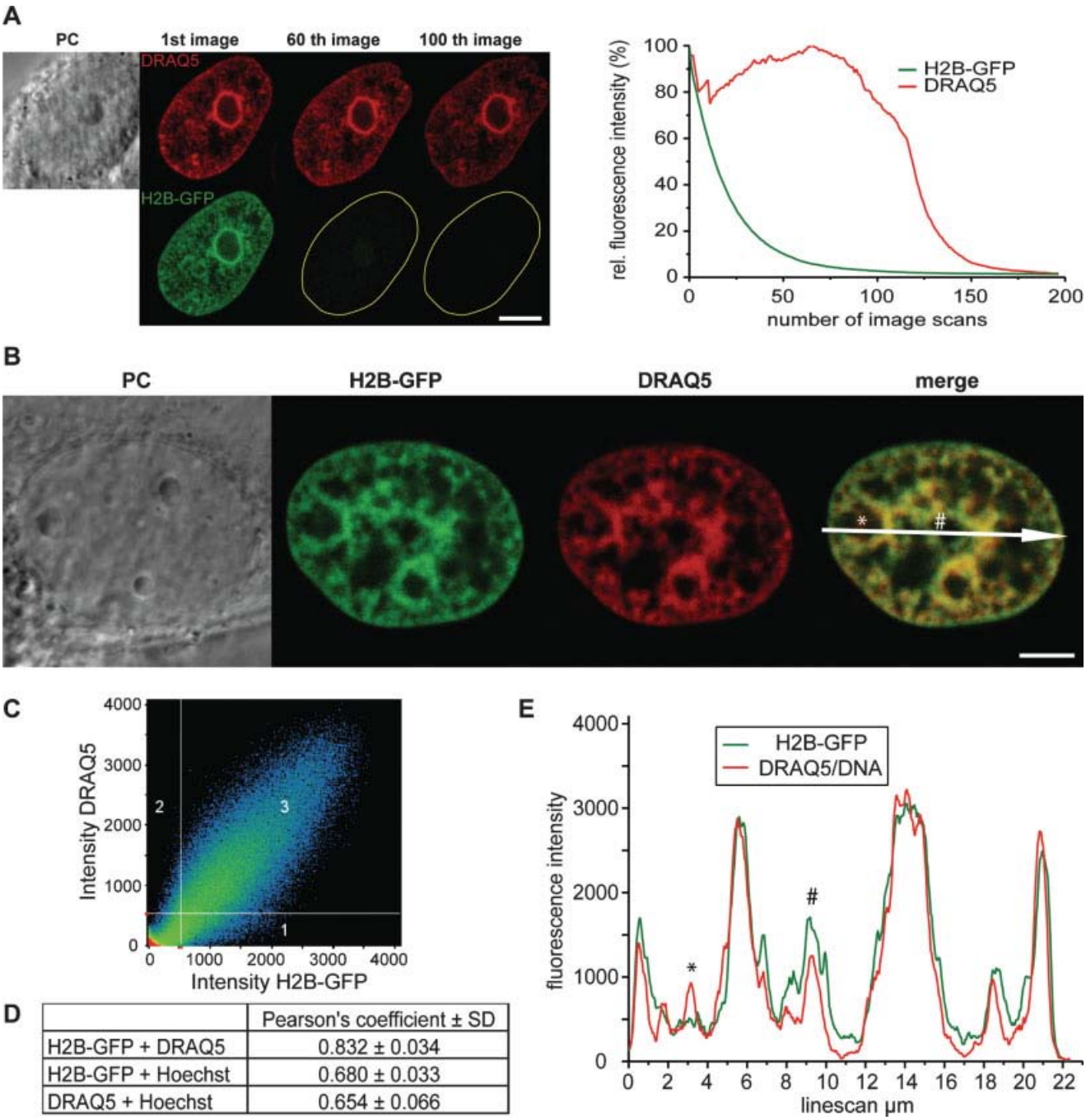

D

	Pearson's coefficient ± SD
H2B-GFP + DRAQ5	0.832 ± 0.034
H2B-GFP + Hoechst	0.680 ± 0.033
DRAQ5 + Hoechst	0.654 ± 0.066

FIG. 3. Quantitative correlation analysis of DNA staining with DRAQ5 versus chromatin labeling with H2B-GFP and comparative photobleaching behavior. **A:** Photobleaching behavior of DRAQ5 versus H2B-GFP. We performed time series with living Hela H2B-GFP cells and acquired 200 images with a confocal microscope in about 30 min to compare the bleaching of both chromatin labels during imaging. The optical sections and the relative mean fluorescence intensity plotted over the number of images showed that the H2B-GFP label completely disappeared after about 60 images, whereas the DRAQ5 signal did not fade substantially until 120 images. DRAQ5 fluorescence even increased in intensity during the time course. **B:** Quantitative correlation analysis of DNA staining with DRAQ5 versus chromatin labeling with H2B-GFP. The image shows a live HeLa H2B-GFP cell stained with DRAQ5 and the almost complete colocalization in the merged image displayed by the yellow color. **E:** Graphs represent the intensity and localization of the two live cell labels along the line in the merged image. The two graphs follow each other in the displayed structures and label intensity. Minor differences can be seen in one nucleolus (*) or in interchromatin regions (#). **C:** The correlation plot describes the pixel colocalization depending on their intensity on the DRAQ5 and H2B-GFP channels with region 3 displaying colocalizing pixels, whereas regions 1 and 2 contain the noncolocalizing pixels for each label, respectively. All signals with intensity below 500 (region under the cross-line) are background. **D:** The distribution of the pixels in region 3 within a thin cone in a 45° angle reveals a very high degree of pixel colocalization and intensity agreement, which is also reflected in the calculated Pearson's coefficient. The same analysis was performed for Hoechst 33258 versus DRAQ5 or H2B-GFP and the respective Pearson's coefficients are presented in D. Scale bar = 5 µm.

compared quantitatively the spatial distribution of both labels by (a) line scan analysis, which displays the pixel intensity on a line of both fluorescence labels, and (b) colocalization analysis describing the overlay of pixels and intensities of both labels. The line scan in Figures 3B and 3E shows that the same nuclear regions are labeled with a similar intensity by DRAQ5 and H2B-GFP. Some minor differences in the label intensity appear in the nucleoli (* in Fig. 3B) where DRAQ5 shows slightly higher signals than H2B-GFP. This observation is most probably due to weak RNA binding by this dye. In other nuclear compartments such as euchromatin or the interchromatin compartment (# in Fig. 3B), the slightly more intense H2B-GFP label could represent unbound and diffuse fluorescent histone fusion proteins. In general, no significant differences between DRAQ5- and H2B-GFP–labeled chromatin structures were observed by line scan analysis (Fig. 3B,E). The same set of images (Fig. 3B) was used for a colocalization analysis of DRAQ5 versus H2B-GFP, which displayed a high degree of pixel colocalization with a Pearson's coefficient of 0.832 ± 0.034 (Fig. 3C,D). In contrast, Hoechst 33258-labeled DNA versus H2B-GFP or DRAQ5 showed only 0.680 ± 0.033 and 0.645 ± 0.066, respectively, reflecting the preferential affinity of Hoechst 33258 to some DNA sequences (Table 1). In summary, at high spatial resolution, DRAQ5 reflects the spatial DNA concentrations in excellent agreement to the chromatin intensity depicted by H2B-GFP.

DISCUSSION

The aim of this work was to find and characterize an easy-to-use live cell DNA stain to label nuclear chromatin compartments for long-term live cell microscopy in combination with the available autofluorescent proteins.

From the five DNA dyes compared, three (PI, TOTO-3, and TOPRO-3) are not suitable for staining living cells, with TOPRO-3 also bleaching very fast (Table 1 and Fig. 1A). Hoechst 33258 can be used to stain DNA in live cells but requires UV excitation, which is toxic to the cells and has a marked preference for A/T-rich sequences, which can bias quantitative studies (1,8). The DNA dye DRAQ5 showed no drastic cytotoxicity effects at 1 μM as the cells slowed down proliferation but did not die (Fig. 2). Decrease of nuclear DNA labeling of the dye visible the next day can be mechanistically related to the efflux of dyes, such as Hoechst 33342 and rhodamine 123, mediated by different ABC transporters reported in multidrug-resistant cells (14,15). These are characterized by high levels of P-glycoprotein, which is responsible for facilitating transport of anticancer drugs out of the cell. DRAQ5 incubation at 1 μM for 24 h did hinder cell cycle progression with accumulation of cells in G2 phase of the cell cycle (Fig. 2). Because this dye is an anthracycline derivative that intercalates into DNA, it is conceivable that it blocks topoisomerase II, thus causing G2 arrest.

Because DRAQ5 is excited with red light and emits deep red fluorescence, it can be used in combination with C/G/YFP and mRFP (Fig. 1B). From our live cell experiments, we can conclude that DRAQ5 is not bleached under normal imaging conditions (Fig. 3A). The labeling of DNA and thereby of chromatin with DRAQ5 is nearly identical with an H2B-GFP label (Fig. 3B-E). Some minor differences in the label intensities could result from a mobile fraction of H2B-GFP, which increases the background in the green channel or the incorporation of histone variants (16). In contrast, DRAQ5 seems to bind to a low extent RNA (13) as seen by a low signal in the nucleoli, which contain mostly rRNAs (Fig. 3B,E).

In contrast to fluorescently tagged histones, DRAQ5 DNA staining does not rely on the transfectability of the cells or the evolutionary conservation of histones and is therefore potentially applicable to all organisms.

Altogether DRAQ5 fulfils several of the requirements for a live cell DNA dye, i.e., it (a) is an easy to use cell-permeant DNA dye, (b) is extremely photostable; (c) allows simultaneous imaging of the available genetically encoded fluorescent proteins, and (d) reflects accurately the spatial concentration of DNA in living cells.

ACKNOWLEDGMENTS

This work was funded by grants from the Deutsche Forschungsgemeinschaft to H.L. and M.C.C. We thank Anje Sporbert for getting us started with the DRAQ5 application and fruitful discussions, Hans-Peter Rahn for help with the FACS analysis, and Alessandro Brero for critical reading of the manuscript. The HeLa H2B-GFP cell line was a generous gift of Kevin Sullivan and the mRFP1 cDNA was kindly provided by Roger Y. Tsien.

LITERATURE CITED

1. Durand RE, Olive PL. Cytotoxicity, mutagenicity and DNA damage by Hoechst 33342. J Histochem Cytochem 1982;30:111–116.
2. Choi M, Rolle S, Wellner M, Cardoso MC, Scheidereit C, Luft FC, Kettritz R. Inhibition of NF-kappaB by a TAT-NEMO-binding domain peptide accelerates constitutive apoptosis and abrogates LPS-delayed neutrophil apoptosis. Blood 2003;102:2259–2267.
3. Suzuki T, Fujikura K, Higashiyama T, Takata K. DNA staining for fluorescence and laser confocal microscopy. J Histochem Cytochem 1997; 45:49–53.
4. Kozubek S, Lukasova E, Amrichova J, Kozubek M, Liskova A, Slotova J. Influence of cell fixation on chromatin topography. Anal Biochem 2000;282:29–38.
5. Haraguchi T, Ding DQ, Yamamoto A, Kaneda T, Koujin T, Hiraoka Y. Multiple-color fluorescence imaging of chromosomes and microtubules in living cells. Cell Struct Funct 1999;24:291–298.
6. Zhang J, Campbell RE, Ting AY, Tsien RY. Creating new fluorescent probes for cell biology. Nat Rev Mol Cell Biol 2002;3:906–918.
7. van Zandvoort MA, de Grauw CJ, Gerritsen HC, Broers JL, Oude Egbrink MG, Ramaekers FC, Slaaf DW. Discrimination of DNA and RNA in cells by a vital fluorescent probe: lifetime imaging of SYTO13 in healthy and apoptotic cells. Cytometry 2002;47:226–235.
8. Davis SK, Bardeen CJ. Cross-linking of histone proteins to DNA by UV illumination of chromatin stained with Hoechst 33342. Photochem Photobiol 2003;77:675–679.
9. Kanda T, Sullivan KF, Wahl GM. Histone-GFP fusion protein enables sensitive analysis of chromosome dynamics in living mammalian cells. Curr Biol 1998;8:377–385.
10. Leonhardt H, Rahn HP, Weinzierl P, Sporbert A, Cremer T, Zink D, Cardoso MC. Dynamics of DNA replication factories in living cells. J Cell Biol 2000;149:271–280.
11. Leonhardt H, Page AW, Weier HU, Bestor TH. A targeting sequence directs DNA methyltransferase to sites of DNA replication in mammalian nuclei. Cell 1992;71:865–873.

12. Smith PJ, Blunt N, Wiltshire M, Hoy T, Teesdale-Spittle P, Craven MR, Watson JV, Amos WB, Errington RJ, Patterson LH. Characteristics of a novel deep red/infrared fluorescent cell-permeant DNA probe, DRAQ5, in intact human cells analyzed by flow cytometry, confocal and multiphoton microscopy. Cytometry 2000;40:280–291.
13. Smith PJ, Wiltshire M, Davies S, Patterson LH, Hoy T. A novel cell permeant and far red-fluorescing DNA probe, DRAQ5, for blood cell discrimination by flow cytometry. J Immunol Methods 1999;229:131–139.
14. Canitrot Y, Lahmy S, Buquen JJ, Canitrot D, Lautier D. Functional study of multidrug resistance with fluorescent dyes. Limits of the assay for low levels of resistance and application in clinical samples. Cancer Lett 1996;106:59–68.
15. Uchida N, Dykstra B, Lyons K, Leung F, Kristiansen M, Eaves C. ABC transporter activities of murine hematopoietic stem cells vary according to their developmental and activation status. Blood 2004;103: 4487–4495.
16. Leach TJ, Mazzeo M, Chotkowski HL, Madigan JP, Wotring MG, Glaser RL. Histone H2A.Z is widely but nonrandomly distributed in chromosomes of Drosophila melanogaster. J Biol Chem 2000;275:23267–23272.